An analytical evaluation of Er:YAG laser cleaning tests on a nineteenth century varnished painting

Chiara Chillè[1], Vassilis M. Papadakis[2], Charis Theodorakopoulos.[1 *]

[1] *Department of Arts, Science in Conservation of Fine Art, Northumbria University, Newcastle upon Tyne, NE1 8ST, UK*
[2] *Institute of Molecular Biology and Biotechnology (IMBB), Foundation for Research and Technology -Hellas (FORTH).*

Abstract
This paper aims to evaluate the Er:YAG laser efficacy to safely thin a varnish on a modern 19th century oil painting. Tests were carried out under single and multiple laser scans directly on the surface (dry) or after pre-wetting with deionised water (DIW) and a non-ionic surfactant (Tween 20), fluence ranges of 0.56-2.40 J/cm^2 and 100 μsec pulse duration. Microscope glass coverslips were placed on the painting surface during irradiation to collect the condensed resin fragments that were extracted from the varnished surfaces. Spectral clusterisation maps of Multispectral Imaging (MSI) data of the irradiated surface supported the evaluation of the procedure. Further evaluation was performed by stereomicroscopy and colourimetry. Fourier Transform Infrared spectroscopy (FT-IR) and Pyrolysis Gas Chromatography / Mass Spectrometry (Py-GC/MS) analysis indicated that the varnish resin was dammar. The collected resin fragments were analysed by FT-IR. The results showed that the resin did not degrade even at the highest level of fluence employed, thereby allowing a subsequent analytical evaluation.

Keywords: Er:YAG laser; Multispectral imaging; Fourier Transform Infrared spectroscopy (FT-IR); Painting.

1. Introduction

The surface cleaning of easel paintings can be considered as one of the most critical, highly sensitive and complex procedure in conservation [1]. This treatment is an irreversible process as it is impossible to reconstitute what was removed from the original painted surface [2].
In the last decades, scientific research in conservation has provided viable alternatives to traditional cleaning methods for paintings, among which there are laser treatments. The first cited work on laser cleaning of paintings was an unpublished report by the Canadian Conservation Institute in 1981 [3].
The interaction of the organic and inorganic paintings' constituents with laser beams and the subsequent removal mechanism of targeted materials, i.e. varnishes, patinas or/and restoration materials, is multifaceted [4]. Recently, the use of the mid-infrared wavelength Er:YAG laser (2940 nm) was successfully tested on easel paintings [5–7], as an alternative to traditional cleaning methods, e.g. the use of solvent admixture or mechanical means.
The aim of this paper is to understand the effects of Er:YAG-induced thinning of a painting's varnish, scanning its surface using one laser pulse per scan and determine the fluence range for a safe varnish irradiation to avoid disruption of the underlying paint layers. In order to address this, a multi-analytical approach was employed. Spectral clusterisation on multispectral imaging data of the treated surfaces areas was carried out to monitor the efficiency of Er:YAG laser cleaning process based on the spectral reflectivity changes across the treated areas. This enables the understanding of the treated surfaces effects including the thinning variations on the varnish layer [8]. For the same reason, colourimetric analysis was also used to determine

*Corresponding author. E-mail address: charis.theodorakopoulos@northumbria.ac.uk (C. Theodorakopoulos).

the impact of laser irradiation to the surface gloss based on factors that were introduced elsewhere [9,10]. Subsequently, Attenuated Total Reflectance / Fourier Transform Infra-Red (ATR/FT-IR) spectroscopy and Pyrolysis Gas Chromatography / Mass Spectroscopy were carried out to characterise the varnish film of the painting prior to the Er:YAG laser irradiation. Then, ATR/FT-IR was performed on the condensed fragments collected on the coverslips upon laser irradiation. Extracting minute quantities of coatings with Er:YAG lasers is a reliable sampling technique for analytical evaluation which has been established elsewhere [6,11–13].

2. Material and methods

2.1 Attenuated Total Reflection / Fourier Transform - Infra-Red Spectroscopy (ATR/FT-IR)

Attenuated Total Reflectance / Fourier Transform - Infra-Red (ATR/FT-IR) Spectroscopy was carried out on a Perkin Elmer bench spectrometer coupled with an FT-IR microscope (PerkinElmer Frontier, Spectrum 400^{TM} FT-IR)[a]. Prior to laser irradiation sampling was conducted under a stereomicroscope by scraping off minor quantities of varnish with a stainless steel scalpel blade No10. The laser irradiated surface was sampled directly during irradiation by collecting the condensed material on glass coverslips, as described below in section 2.3, which is an established micro-destructive sampling technique [6,11–13]. Samples of the untreated and treated varnish were placed directly on the diamond window and pressed (up to pressure gauge of 110). The working wavenumber range was from 4000 to 380 cm^{-1}, and the spectra were acquired at 16 scans at 4 cm^{-1} resolution. The background was automatically subtracted. The ATR/FT-IR spectra were processed using PerkinElmer Spectrum^{TM} 10 software suite. The integrated areas of the peaks corresponding to stretching vibrations of hydroxide (2700-3700 cm^{-1}), C-H (2850-3000 cm^{-1}) and carbonyl (1500-1900 cm^{-1}) bonds were determined [14]. These spectra were normalised to an identical intensity at the C-H stretching frequency of 2953 cm^{-1} [15]. Consequently, the ratios of the integrated areas of the selected OH/CH and the C=O/CH band were determined. The generated data were compared to the non-irradiated sample to monitor any possible chemical changes after laser irradiation.

2.2 Pyrolysis - TMAH- Gas Chromatography / Mass Spectroscopy (Py-TMAH-GC/MS)

Pyrolysis - Gas Chromatography / Mass Spectrometry was carried out on a Thermo Finnigan Focus GC Gas Chromatograph with an Agilent DB5-MS UI column (ID: 0.25 mm, length: 30 m, df: 0.25 μm, Agilent, Santa Clara, CA, USA), fitted with a Pyrola 2000 Platinum filament pyrolyser (PyroLab, Sweden). A sample of the order of 0.5 mg was directly derivatised in an aliquot of 1 μl of 25wt% in methanol tetramethylammonium hydroxide (TMAH) and placed on the Pt filament. The Pyrolyser was coupled to a DSQII Mass Spectrometer. The inlet temperature to the GC was kept at 280 °C. The helium carrier gas flow rate was 1 ml/min with a split flow of 13 ml/min. The MS transfer line was held at 280 °C and the ion source at 250 °C. The pyrolysis chamber was heated to 175 °C, and pyrolysis was carried out at 600 °C for 2s for the majority of samples. The temperature program was set as follows: 40 °C for 2 mins followed by 26 mins of 8 °C/min to 250 °C followed by 10 mins of 3 °C/min up to 280 °C, and a final step at 280°C held for 20 mins to a total run time of 58 mins. Acquisition was carried out in a Total Ion Count mode, where all ions in the range 40-800 m/z were monitored. The data were examined and processed using Thermo Scientific Xcalibur^{TM} 2.2 version. Characterisation was verified with previous findings [16–20].

2.3 Laser Cleaning Tests

A Fotona Fidelis^{XS}, VSP Er:YAG laser (λ = 2.94 μm) in Very Short Pulse (VSP) mode (laser pulse duration (τ_p)≈ 100 μsec) was employed. The laser was equipped with an articulated mirror arm and was operated in the free-running mode. The beam was delivered perpendicularly onto the varnish surface by a straight collimated full-beam titanium handpiece R11, held by the laser-operator like a pen. The laser beam diameter was set at 3 mm, both in the handpiece and in the Fidelis^{TM} display, and the pulse repetition rate was set at 2 Hz.

A Fotona XS Dynamis Er:YAG laser in the VSP mode was employed to determine the laser working distance and the laser beam diameter prior to the laser cleaning tests on the painting. A titanium handpiece R11 was fixed at three different working distances: 2, 5 and 10 cm. The distances were measured from the lens at the end of the handpiece up to the surface of a photosensitive black paper. The laser beam was released to create a series of laser beam spots on the paper. The laser spot areas were calculated and fluences were determined by dividing the laser energy by the measured spot areas. Each manually determined fluence was compared to fluence reading on the Fidelis^{TM} display (Fig. S1).
The laser irradiation tests were carried out in fluences, as shown in the laser unit display, ranging from 0.6 to 2.4 J/cm^{2}[b], from this point on the fluence values would be referred to as "nominated fluences". The working distance measured between the end of the handpiece and the painting surface (nineteenth century easel painting, size: 95 x 54 cm) was kept constant at 5 cm. Single and multiple laser pulses were fired onto the painting surface, creating a total of twenty-two tested areas (Fig. 1). In each of them, six different tests were run (15x15 mm squares) (Fig. 2), at first on the dry-irradiated surface and then using five different wetting agents, which were:

- Deionised Water (DIW);
- 1% (v/v) of non-ionic surfactant (Tween®20[c]) in 50 mL of Deionised water (DIW+TW20) [1];
- 50 (%v/v) Industrial Methylated Spirit (IMS[d]) in deionised water (50% IMS+DIW);
- 50 (%v/v) IMS and White Spirit (WS[e]) (50% IMS+WS);
- White Spirit (WS).

These solvents and solutions employed were thoughtfully selected to monitor the interaction of the laser with various surface polarities[f][12] by using Cremonesi-Wolbers solubility tests [1,21]. According to the latter tests, binary solvent mixtures, composed of WS and acetone or WS and IMS, were used at various concentrations [1,7] in order to monitor the polarity threshold for the efficient solubilisation of the varnish film. Furthermore, the Fractional Solubility Parameter provided an indication of the surface polarity and it was calculated for each of the agents[g].
Prior to the laser irradiation of the varnish surface, all the glass coverslips (15x15 mm) were cleaned using deionised water, acetone, ethanol and then dried.
For the pre-wetting procedure, the painting surface was wetted with cotton swabs. The latter loaded with wetting agents were firstly drained on a blotting paper before the swabs were rolled three times on the varnish surface. Then, the area was immediately covered with thin glass coverslips and irradiated with the laser. Considering practicalities and previous trials [12], for tests based on two laser scans, the varnish surface was pre-wetted at the beginning of each laser scan. For trials based on three laser scans, the varnish layer was pre-wetted only once prior to laser irradiations.

2.4 Studio photography

The twenty-two test areas were photographed using a Canon digital camera Compact-Macro Lens 50mm 1:2,5 fixed/prime. Each set was captured before and after laser irradiation in the same lighting conditions using visible (VIS) daylight and ultraviolet (UV) lamps. VIS: Bowens SL855 with 8 daylight light (approximately 5800 K) sources provided illumination in the visible and near-infrared regions. UV lamps (UV 72W blacklight) had an emission between 315 and 400 nm (peak 365 nm). A Kodak Wratten 2E filter cutting off wavelengths below 415 nm was employed for the UV induced fluorescence imaging.

2.5 Stereomicroscopy

Stereomicroscopic observations of the painting surface were carried out before and after laser irradiations in reflected light with a Leica Stereo Zoom S6 D 6.3:1 stereomicroscope (6.3x - 20x magnification) that provides a field of view up to 36.5 mm. A Leica MC170 HD

Microscope Camera (5 Megapixel HD) and a set of LED fibre optic lights were employed to capture the micrographs.

2.6 Colourimetry

Colourimetric measurements were carried out with a Konica Minolta Spectrophotometer CM 2600-D covering a 360–740 nm spectral range at spectral resolution of 10 nm. The spot diameter was set at 3 mm, using a Target Mask CM-A147. The data were acquired in both Specular Component Included (SCI) and Specular Component Excluded (SCE) modes. Three measurements for each examined area (inside the laser-treated tests and outside near the edge of the untreated areas) were averaged to obtain each data point. The data used for this study were the lightness values L* ranging between 100 (brightest white) and 0 (darkest black) acquired in SCI and SCE modes [9,10,22]. In SCE mode a glossy surface returns values closer to zero (darker) than a matte surface of the same colour [22].

According to Kun et al. (2014) [9] and Sanderson et al. (2015) [10], SCI = SCE+GRF (Gloss Related Factor). Thus, the change in the painting's surface, before and after laser irradiation, was calculated by the following formulas:

$$GRF_b = L^*_{SCI_b} - L^*_{SCE_b} \quad \text{(Eq. 1)}$$

$$GRF_a = L^*_{SCI_a} - L^*_{SCE_a} \quad \text{(Eq. 2)}$$

where indices b and a correspond values before and after irradiation, respectively. Therefore, the irradiation impact to the surface gloss can be determined as:

$$\Delta GRF = GRF_b - GRF_a \quad \text{(Eq. 3)}$$

Herein, the surface was not further processed with any solution after laser irradiation, which is common in art conservation procedures [7].

2.7 Multispectral imaging

Multispectral Imaging (MSI) was performed using an XpeCAM X01 camera (XpectralTEK). The device, equipped with a 5M pixels monochrome CMOS sensor, and a 35 mm / F1.3 objective lens, acquired a sequence of spectral images ranging from 350 - 400 nm every 10 nm, 400 - 700 nm every 25 nm and 700 - 1200 nm every 50 nm. The same light sources as those for studio photography were employed. A white Diffuse Reflectance Target (DRT) was used for calibration purposes. The DRT was placed very close and parallel to the painting surface, enabling spectral intensity calibration and corrections for inhomogeneous illuminance of the surface. Acquisition was performed for both DRT and sample images. Each spectral image was then normalised with the corresponding DRT spectral image. MSI data were processed with an advanced image-processing programme, Tensor Image Processing Platform (TIPP), specifically designed to analyse MSI data[hi]. The acquired spectral images were then processed by a blind clustering method (k-means clusterisation) [23], where individual pixel spectral similarities were mapped with a single colour. Spectral clustering was carried out on 11 spectral images in the 360 - 550 nm wavelength range, in which the aged varnish absorbed strongly (Fig. S1). Distinct areas were classified by significant reflectance differences. The generated MSI clusterisation maps provided information related to the percentage of the varnish thinning. Quantification of the laser irradiation efficacy was performed via calculation of the clusters' surface coverage, in each scanned area.

3. Results and Discussion

3.1 Varnish Characterisation

Prior to the laser irradiation tests, the varnish of the painting was characterised by means of ATR/FT-IR and Py-TMAH-GC/MS, which showed that it was a triterpenoid (TTP) dammar resin varnish. The ATR/FT-IR spectra are reported in Fig. 3 and their frequency assignments are listed in Table 1. The presence of the broad absorbance band at 3400 cm^{-1} corresponding to 2940 nm, attributed to stretching vibrations of O-H groups, indicates the absorption at the

Er:YAG laser wavelength [5]. Methyl and methylene groups gave two sharp absorption peaks at 2943 and 2875 cm^{-1} due to asymmetric CH_3/CH_2 and symmetric CH_3 stretching, while 1453 and 1380 cm^{-1} peak were attributed to the C–H bending of CH_2 and CH_3, respectively [24,25]. The triterpenoid varnish painting sample showed a characteristic IR absorbance peak at 1705 cm^{-1}, due to the C=O carbonyl stretching vibration of the resinous acids [26]. The band at 1630 cm^{-1} corresponded to the C=C stretching, 1165 cm^{-1} and 1236 cm^{-1} were attributed to the saturated C–C stretching vibrations. The peak at 874 cm^{-1} indicated CH out-of-plane deformation of two hydrogen atoms in aromatic rings [24]. The chromatogram of the Py-TMAH-GC/MS study showed a series of peaks between 35 and 58 minutes (Fig. 4) correspond to a TTP resin. The main peaks were identified in the mass spectra as *dammaradienone*, *dammaradienol*, *dammarenolic acid*, *oleanonic acid*, *hydroxydammarenone*, *oleanonic aldehyde*, *ursonic acid* and *ursonic aldehyde* (Table 2, Figs. S3-S10). The presence of dammarenolic and ursonic acids (Figs. S5 and S9) indicated that the resin was dammar [16,17,19,24,27,28].

3.2 Er:YAG Laser tests

The procedure for the Er:YAG laser tests was carried out on a 19th century modern oil painting to breakdown and thin the dammar varnish without removing it (Fig. 1). A gradual increase in the nominated fluence was used, and coverslips were placed in between the paint surface and the handpiece to collect resin fragments for further analyses. Laser irradiation run both on dry surface and with wetting agents, ranging from auxiliary OH-containing solvents (such as DIW and IMS) to a non-OH solvent (WS). Since the efficiency of the Er:YAG laser is directly proportional to the number of OH groups present in the surface [29], hydroxides were introduced by adding hydroxylated liquids, which aided to increase the laser interaction with the varnish layer [11,30], therefore reducing the heat diffusion of the incident 2.94 μm beam in the bulk [5,31,32]. Laser irradiation resulted in circular spots that were identified on the dammar varnish surface. The spots were gradually more defined when increasing the nominated fluence[j]. Due to this effect, the gloss of the varnish surface was progressively reduced to a whitish appearance also because of augmented light scattering.

The tests showed that irradiation of the varnish had similar results[k] when the surface was: a) dry or pre-wetted with WS, b) pre-wetted with DIW and DIW+TW20, and c) pre-wetted with 50% IMS+WS and 50% IMS+DIW. As reported in section 2.3, Cremonesi-Wolbers solubility tests [1,21] were carried out on the painting prior to irradiation. Specifically, by comparing the values of non-polar dispersion forces, f_d, polar dipole forces, f_p, and hydrogen bond forces, f_h, the presence of a natural resin varnish was determined [1,33–35]. The test of solubility carried out before the laser test revealed that neat IMS could have partially solubilised the varnish. For this reason, the data discussed in this paper were those of the dry irradiated and the DIW+TW20 pre-wetted tests to evaluate the Er:YAG laser efficacy to safely interact with the varnish layers. Nominated fluences between 0.7 and 2.4 J/cm^2 generated an evident breakdown of the surface, and the tests proceeded with one, two and three laser scans (Figs. 5 and 6). The varnish thinning was verified by detecting the condensed material on the coverslips and by visually assessing the painting surface under visible and UV light.

In correspondence to the dry irradiation tests, the desired outcome was obtained by one scan at 2 J/cm^2 and two scans at nominated fluences ranging from 0.7-1 J/cm^2 with no apparent colour variation of the varnish surface by eye (Fig. 5). An over-treatment, identified as the generation of a brown hue of the irradiated area, was visually assessed after one laser scan at 2.1 J/cm^2, as well as at two laser scans of the surface at 1 J/cm^2 using the stereomicroscope. This visually assessed colour variation can be related to laser-induced photothermal and photomechanical effects [6,29,31,36]. Satisfying results in terms of a gradual thinning of the varnish without a brownish discolouration were obtained in the presence of DIW+TW20 at one laser scan at 2.4 J/cm^2, two laser scans applications at 2.3 J/cm^2 and three laser scans applications at 2.1 J/cm^2, respectively (Fig. 6, Table 3).

Furthermore, all the tested areas developed a change in the surface morphology of the irradiated varnish, which showed the formation of micro-roughness (Fig. 5 III and Fig. 6 III), as also discussed elsewhere [30,31,36]. The tests showed that dry irradiation resulted in the collection of more resin fragments on the cover slips than the pre-wet tests at the same laser settings (Fig. 7).

3.3 Colourimetric measurements

Colourimetry allowed to assess a consistent increase in lightness L^* in SCI and SCE modes for the tested areas after laser irradiation (Table 3). This increase in L^*, being this parameter related both to the increased light scattering and therefore to the increased brightness of the varnish, confirmed the visually observed whitening of the irradiated varnish and its disruption induced by laser irradiation. L^*_{SCI} and L^*_{SCE} values before and after laser irradiation, were employed to determine the gloss related factors, GRF_b and GRF_a (Eq. 1 and 2). Thus, the ΔGRF (Eq. 3) determines the impact due to laser irradiation, corresponding to the reduction in gloss of the surface (Table 3 and Fig. 8).

The plot in Figure 7 shows that the dry irradiated areas with one laser scan had a higher ΔGRF value compared to the two laser scanned areas. It is possible to observe a considerable gap between the area scanned once with the area scanned twice, except for the areas irradiated at 0.6 J/cm^2 due to the weak laser interaction with the varnish surface. By increasing the fluence, in the dry irradiated areas with one laser scan, an increasing trend in the interaction is detected with a maximum at 2 J/cm^2 followed by a decrement. The same pattern is observed in the two times scanned areas with a peak at 1 J/cm^2. In this plot it is possible to identify a good correlation between the maximum ΔGRF value with the desired outcome that was visually assessed for the one laser scan areas at 2 J/cm^2 (Fig. 5). In the case of the two laser scanned areas, the maximum ΔGRF is obtained at about 1 J/cm^2, which is in agreement with the post-irradiation visual assessment of the surface.

A similar comparison is made in the ΔGRF values of the prewetted surfaces at one and two scans, where the values of the one scan surfaces are higher than the values for the two scans. In this case, the ΔGRF data of the one scan areas remain almost stable up to 1.5 J/cm^2 and significantly increase at 2 J/cm^2. ΔGRF data of the two scanned prewetted areas are almost stable at all fluences. The three scanned prewetted areas could not be compared here because these areas were only prewetted once prior to irradiation which caused significant light scattering at the varnish surface compared to the one- and two-scanned areas. However, the data are reported in table 3.

These results along with UV fluorescence findings were combined with multispectral imaging data to further evaluate the efficacy of the Er:YAG laser irradiation (Table 4).

3.4 Multispectral imaging

Following irradiation, the thickness of the remaining varnish layer, presented a high variability. Spectral clusterisation resulted to 3 clusters depicted in different colours (Fig. 9). Black colour corresponds to the non-irradiated varnish. Green represents an early-stage varnish thinning, while red represents a gradual deeper reduction, resulting in a thinner remaining varnish layer. The absorption of the varnish is dependent on its physical and chemical characteristics, such as its thickness and the concentration of compounds with light absorbing functional groups, such as those generated in degradation products in dammar resin due to ageing [37,38]. The study of the spectral image sets, in the scanned areas, showed that up to 425 nm the reflectance was exclusively due to the varnish layer (Fig. S2). Upon ageing, dammar varnishes absorb strongly not only in the UV but also in the blue part of the visible spectrum (400-490 nm) due to the presence of unsaturated quinines [24,37,39]. Thus, background reflectance is minimised due to

the strong absorption of the varnish in the blue, as also is evidenced in the presented case (Fig. S1).
However, in order to negate any contribution from underlying paint layer in the scanned areas, the ratio between the average reflectance spectra of the red and green clusters was determined (Fig. 10). Considering that the green and red clusters represent raster of scattered points of thicker and thinner films of the remaining varnish, this ratio clearly represents the reflectance difference due to thickness. A similar approach was previously reported to monitor the thickness of black crust layers on marble substrates [40].
Fig. 10 shows the similar spectral characteristics of the irradiated varnish regardless of the pre-wet or dry irradiated procedure. In the two laser scanned pre-wetted and dry areas the ratios of the green over red clusters resulted in identical spectra, providing further evidence that no contribution from the background was detected. This is also due to the fact that the two laser scanned areas, regardless of pre-wetting, were processed with the same method as reported in section 2.3. Regardless of scattering which offsets the spectra in Fig. 10, it can be seen that the aged varnish reflected strongly at 380 nm and that by increasing the laser scans, and therefore gradually thinning the varnish layer, a stronger reflectance at 370 nm was eventually recorded. The gradual reflectance shift from 380 nm to 370 nm is in line with previous findings on UV/VIS spectrophotometry of TTP resins thinned with excimer lasers [24]. In this spectral region, tails of the carbonyl groups of hydroperoxides, aliphatic acids, and aldehydes with peak absorption at wavelengths below 250 nm, affect the UV absorption and reflection of the films due to n $\rightarrow\pi^*$ transitions [41]. Moreover, absorbance in the near UV is gradually shifted towards shorter UV wavelengths as function of depth [24], which was verified in the presented study (Fig. 10). In addition to the aforementioned information, the clusterisation maps (Fig. 9) indicated that the interactions of the dry and pre-wetted varnish with the laser were different and determined the progressive thinning of the varnish layer.

The percentage surface coverage of the clusters of the dry and the DIW+TW20 irradiated areas as a function of nominated fluence showed that pre-wetting the surface results in a more controlled interaction (Fig. 11). In particular, the dry irradiated surface presented an abrupt thinning of the varnish with lower fluencies. For instance, 2 scans at the dry irradiation procedure maximised the varnish thinning abruptly between 0.6 and 0.7 J/cm^2, contrary to the pre-wet procedure where a similar result was obtained more gradually in a higher nominated fluence range from 1 to 2 J/cm^2. Thus, this study indicates that pre-wetting offers a more controlled and gentle interaction.

3.5 Further Spectroscopic Evaluation
The ATR/FT-IR spectra obtained from the residual varnish collected on the coverslips (acquired at different nominated fluences) upon laser irradiation were therefore compared with the varnish sample that was not irradiated (Fig. 12). Given that resin fragment were directly extracted from the glass coverslips the results were not affected as in the case of the visual interpretation due to light scattering at the surface of the irradiated varnish, as observed on the three-scanned areas. The ratios of the integrated areas of the OH/CH and the C=O/CH bands did not show significant changes in dry and pre-wet mode after scanning the surface one time. However, it was possible to detect small differences in the varnish after two or three laser scans irradiations. The absorbance band at 3700-3100 cm^{-1} attributed to OH stretching vibrations showed no changes in intensity also at the highest nominated fluence at 2.1 J/cm^2 in all tests. Conversely, the intensity of the carbonyl stretching vibration band gradually decreased by increasing the nominated fluence (Fig. 12), as was also observed in KrF excimer laser ablated triterpenoid varnishes [24,42]. Taking it all into account, there was not a considerable modification in the OH/CH and C=O/CH ratios of the treated varnish fragments by increasing the nominated fluence. However, the lightly decrease in the carbonyl stretching vibration has suggested the presence of a degradation gradients in the triterpenoid varnish [24,42].

4. Conclusions

This paper provides an example where an Er:YAG laser was used to thin a dammar varnish of an oil painting, as evidenced by ATR/FT-IR and py-TMAH-GC/MS. Laser irradiation tests led to diverse results depending on whether the surface was directly irradiated dry or pre-wetted with deionised water with a non-ionic surfactant. The tests were effective in the nominated fluences ranging from 1 to 2.4 J/cm^2 in one, two and three laser scan applications. Multispectral imaging clusterisation maps of the tested areas were particularly useful for the evaluation and monitoring of the laser effects to the surface.

A gloss related impact due to irradiation was in good agreement with the visual assessment of the post-treated surface. Furthermore, ATR/FT-IR spectra carried out on the resin scrapings assessed the laser cleaning efficiency process by monitoring the changes in the OH/CH and C=O/CH ratios. Laser irradiation did not show a considerable modification in the abovementioned ratios. The minor decrease in the C=O/CH ratios, however, indicated that the dammar varnish was less deteriorated in the bulk than in the surface [42]. Overall, this work supplied an insight into the mechanism of the Er:YAG laser irradiation of varnished paintings. This alternative method can enable the conservator to address a cleaning procedure using less invasive and safer techniques when laser irradiation is used within appropriate energy levels.

Acknowledgement

The authors acknowledge Ed Teppo (founder and president of former Enterprise Big Sky Laser Technologies) for lending the Fotona FidelisXS Er:YAG laser to the Northumbria University Art Conservation Laboratory and for the laser spots analysis. Also special thanks to XpectralTEK LDA for providing the XpeCAM X01 multispectral system and the software tools used for the study. This research is sponsored by RDF Northumbria Research Support.

References

[1] P. Cremonesi, E. Signorini, Un approccio alla pulitura dei dipinti mobili, Il Prato, Saonara, Italy, 2012.

[2] A. Oddy, Does reversibility exist in conservation?, in: A. Oddy, S. Carroll (Eds.), Reversibility - Does It Exist., British Museum, London, 1999: pp. 1–5.

[3] L. Carlyle, Laser Interactions with Paintings: Results and Proposals for Further Study, Unpubl. Report, Ottawa Can. Conserv. Inst. (1981).

[4] A. DeCruz, A. Andreotti, A. Ceccarini, M.P. Colombini, Laser cleaning of works of art: evaluation of the thermal stress induced by Er:YAG laser, Appl. Phys. B Lasers Opt. 117 (2014) 533–541. doi:10.1007/s00340-014-5865-3.

[5] A. Andreotti, W.P. Brown, M. Camaiti, M.P. Colombini, A. DeCruz, Diagnosis of materials and effectiveness of Er:YAG laser cleaning as complementary treatment in a panel painting attributed to Lluís Borrassà (fifteenth century), Appl. Phys. A. 122 (2016) 572. doi:10.1007/s00339-016-0100-1.

[6] A. Andreotti, P. Bracco, M.P. Colombini, A. DeCruz, G. Lanterna, K. Nakahara, F. Penaglia, Novel Applications of the Er:YAG Laser Cleaning of Old Paintings, in: J. Nimmrichter, W. Kautek, M. Schreiner (Eds.), Lasers Conserv. Artworks, Proc. Lacona VI, Vienna, Austria, Sept 21-25, 2005, Springer, Berlin, Heidelberg, 2007: pp. 239–247. doi:10.1007/978-3-540-72130-7_28.

[7] A. Brunetto, G. Bono, F. Frezzato, Er : YAG laser cleaning of ‘ San Marziale in Gloria ’ by Jacopo Tintoretto in the Church of San Marziale , Venice, J. Inst. Conserv. 43 (2020) 1–15. doi:10.1080/19455224.2019.1706596.

[8] V. Papadakis, A. Loukaiti, P. Pouli, A spectral imaging methodology for determining on-line the optimum cleaning level of stonework, J. Cult. Herit. 11 (2010) 325–328.

doi:10.1016/j.culher.2009.10.007.
[9] Y. Kun, Y. Huimin, J. Shangzhong, A type of spectrophotometer with both SCI and SCE measurement structures, Optik (Stuttg). 125 (2014) 4672–4677. doi:10.1016/j.ijleo.2014.04.089.
[10] K. Sanderson, A Comparative Study of Handheld Reflectance Spectrophotometers, Top. Photogr. Preserv. AIC Annu. Meet. San Fr. 2014. 16 (2015) 47–62.
[11] M.P. Colombini, A. Andreotti, G. Lanterna, M. Rizzi, A novel approach for high selective micro-sampling of organic painting materials by Er:YAG laser ablation, J. Cult. Herit. 4 (2003) 355s-361s. doi:10.1016/S1296-2074(02)01218-9.
[12] P. Bracco, G. Lanterna, M. Matteini, K. Nakahara, O. Sartiani, A. DeCruz, M.L. Wolbarsht, E. Adamkiewicz, M.P. Colombini, Er:YAG laser: an innovative tool for controlled cleaning of old paintings: testing and evaluation, J. Cult. Herit. 4 (2003) 202–208. doi:10.1016/S1296-2074(02)01232-3.
[13] A. Andreotti, M.P. Colombini, A. DeCruz, Er:YAG laser cleaning of a marble Roman urn, J. Inst. Conserv. 43 (2020) 12–24. doi:10.1080/19455224.2019.1706593.
[14] D. Ciofini, Removal Of Varnish And Overpaint Layers From Easel Paintings Using Pulsed Nd:YAG Lasers, Doctoral dissertation, University of Florence, 2014.
[15] M. Derrick, D. Stulik, J. Landry, Infrared spectroscopy in conservation science, The Getty Conservation Institute, Los Angeles, 1999. doi:10.1017/CBO9781107415324.004.
[16] S. Watts, E.R. de la Rie, Gcms Analysis of Triterpenoid Resins: In Situ Derivatization Procedures Using Quaternary Ammonium Hydroxides, Stud. Conserv. 47 (2002) 257–272. doi:10.1179/sic.2002.47.4.257.
[17] M.P. Colombini, F. Modugno, S. Giannarelli, R. Fuoco, M. Matteini, GC-MS characterization of paint varnishes, Microchem. J. 67 (2000) 385–396. doi:10.1016/S0026-265X(00)00098-9.
[18] G.A. van der Doelen, K.J. van den Berg, J.J. Boon, Comparative chromatographic and mass-spectrometric studies of triterpenoid varnishes: fresh material and aged samples from paintings, Stud. Conserv. 43 (1998) 249–264. doi:10.1179/sic.1998.43.4.249.
[19] G.A. van der Doelen, K.J. van den Berg, J.J. Boon, N. Shibayama, E.R. de la Rie, W.J.L. Genuit, Analysis of fresh triterpenoid resins and aged triterpenoid varnishes by high-performance liquid chromatography-atmospheric pressure chemical ionisation (tandem) mass spectrometry, J. Chromatogr. A. 809 (1998) 21–37. doi:10.1016/S0021-9673(98)00186-1.
[20] C. Theodorakopoulos, J.J. Boon, V. Zafiropulos, Direct temperature mass spectrometric study on the depth-dependent compositional gradients of aged triterpenoid varnishes, Int. J. Mass Spectrom. 284 (2009) 98–107. doi:10.1016/j.ijms.2008.11.004.
[21] R. Wolbers, Cleaning painted surfaces : aqueous methods, Archetype Publications, London, 2000.
[22] T. Mouw, Specular Included or Specular Excluded: Which is Best?, X-Rite Blog. (2018). https://www.xrite.com/blog/specular-included-or-specular-excluded-which-is-best?utm_source=google&utm_medium=cpc&utm_campaign=03-GO-GB-EN-DSA&utm_content=DSA_Website&utm_term=&matchtype=b&device=c&gclid=Cj0KCQjwmpb0BRCBARIsAG7y4zbfWs3j-AaD7f03TdfLeYVibFQt (accessed April 14, 2020).
[23] C. Ding, X. He, H.D. Simon, Nonnegative Lagrangian Relaxation of K-Means and Spectral Clustering, in: J. Gama, R. Camacho, P.B. Brazdil, A.M. Jorge, L. Torgo (Eds.), Mach. Learn. ECML 2005. ECML 2005. Lect. Notes Comput. Sci. Vol 3720, Springer, Berlin, Heidelberg, 2005: pp. 530–538. doi:10.1007/11564096_51.
[24] C. Theodorakopoulos, V. Zafiropulos, J.J. Boon, S.C. Boyatzis, Spectroscopic Investigations on the Depth-Dependent Degradation Gradients of Aged Triterpenoid Varnishes, Appl. Spectrosc. 61 (2007) 1045–1051. doi:10.1366/000370207782217833.

[25] M.V. Russo, P. Avino, Characterization and Identification of Natural Terpenic Resins employed in “Madonna con Bambino e Angeli” by Antonello da Messina using Gas Chromatography-Mass Spectrometry., Chem. Cent. J. 6 (2012) 59. doi:10.1186/1752-153X-6-59.
[26] C. Invernizzi, T. Rovetta, M. Licchelli, M. Malagodi, Mid and near-infrared reflection spectral database of natural organic materials in the cultural heritage field, Int. J. Anal. Chem. 2018 (2018). doi:10.1155/2018/7823248.
[27] I. Bonaduce, F. Di Girolamo, I. Corsi, I. Degano, M.R. Tinè, M.P. Colombini, Terpenoid Oligomers of Dammar Resin, J. Nat. Prod. 79 (2016) 845–856. doi:10.1021/acs.jnatprod.5b00916.
[28] P. Dietemann, C. Higgitt, M. Kälin, M.J. Edelmann, R. Knochenmuss, R. Zenobi, Aging and yellowing of triterpenoid resin varnishes - Influence of aging conditions and resin composition, J. Cult. Herit. 10 (2009) 30–40. doi:10.1016/j.culher.2008.04.007.
[29] L. Pereira-Pardo, C. Korenberg, The use of erbium lasers for the conservation of cultural heritage. A review, J. Cult. Herit. 31 (2018) 236–247. doi:10.1016/j.culher.2017.10.007.
[30] E. Teppo, Introduction: Er:YAG lasers in the conservation of artworks, J. Inst. Conserv. 43 (2020) 1–10. doi:10.1080/19455224.2019.1706597.
[31] C. Chillè, F. Sala, Q. Wu, C. Theodorakopoulos, A study on the heat distribution and oxidative modification of aged dammar films upon Er : YAG laser irradiation A study on the heat distribution and oxidative irradiation, J. Inst. Conserv. 43 (2020) 1–20. doi:10.1080/19455224.2019.1707699.
[32] A. DeCruz, M.L. Wolbarsht, S.A. Hauger, Laser removal of contaminants from painted surfaces, J. Cult. Herit. 1 (2000) S173–S180. doi:10.1016/S1296-2074(00)00182-5.
[33] J. Striber, V. Jovanović, M. Jovanović, Easel paintings on canvas and panel: application of Nd:YAG laser at 355 nm, 1064 nm and UV, IR and visible light for the development of new methodologies in conservation, in: P. Targowski, M. Walczak, P. Pouli (Eds.), Proc. Int. Conf. LACONA XI, Nicolaus Copernicus University Press, Toruń, 2017: pp. 279–292. doi:10.12775/3875-4.20.
[34] J.P. Teas, Graphic analysis of resin solubilities, J. Paint Technol. 40 (1968) 19–25.
[35] A. Phenix, Effects of Organic Solvents on Artists’ Oil Paint Films: Swelling, in: M.F. Mecklenburg, A.E. Charola, R.J. Koestler (Eds.), New Insights into Clean. Paint. Proc. from Clean. 2010 Int. Conf. Univ. Politécnica Val. Museum Conserv. Inst., Smithsonian Institution Scholarly Press, Washington, DC., 2013: pp. 69–76.
[36] M. Lopez, X. Bai, C. Koch-Dandolo, S. Serfaty, N. Wilkie-Chancellier, V. Detalle, Nd:YAG vs Er:YAG : a comparative study of laser varnish removal on easel paintings, in: P. Targowski, R. Groves, H. Liang (Eds.), Opt. Arts, Archit. Archaeol. VII, SPIE, 2019: p. 3. doi:10.1117/12.2527437.
[37] M.W. Formo, Physical Properties of Fats and Fatty Acids, in: D. Swern (Ed.), Bailey’s Ind. Oil Fat Prod. Vol. 1, 4th ed, John Wiley & Sons, Ltd, New York, NY, USA, 1979.
[38] G.A. van der Doelen, J.J. Boon, Artificial ageing of varnish triterpenoids in solution, J. Photochem. Photobiol. A Chem. 134 (2000) 45–57. doi:10.1016/S1010-6030(00)00245-8.
[39] E.R. de la Rie, Photochemical and thermal degradation of films of dammar resin, Stud. Conserv. 33 (1988) 53–70. doi:10.1179/sic.1988.33.2.53.
[40] V.M. Papadakis, Y. Orphanos, S. Kogou, K. Melessanaki, P. Pouli, C. Fotakis, IRIS: a novel spectral imaging system for the analysis of cultural heritage objects, in: SPIE Opt. Metrol. Munich, Ger. Proc. Vol. 8084, O3A Opt. Arts, Archit. Archaeol. III; 80840W, 2011: p. 80840W. doi:10.1117/12.889510.
[41] R.M. Silverstein, G.C. Bassler, T.C. Morrill, Spectrometric identification of organic compounds, 5th ed., John Wiley & Sons, Ltd, New York, 1991.
[42] C. Theodorakopoulos, V. Zafiropulos, Uncovering of scalar oxidation within naturally aged varnish layers, J. Cult. Herit. 4 (2003) 216–222. doi:10.1016/S1296-

2074(02)01200-1.
[43] D. Ciofini, J. Striova, M. Camaiti, S. Siano, Photo-oxidative kinetics of solvent and oil-based terpenoid varnishes, Polym. Degrad. Stab. 123 (2016) 47–61. doi:10.1016/j.polymdegradstab.2015.11.002.
[44] A. Zacharopoulos, K. Hatzigiannakis, P. Karamaoynas, V.M. Papadakis, M. Andrianakis, K. Melessanaki, X. Zabulis, A method for the registration of spectral images of paintings and its evaluation, J. Cult. Herit. 29 (2018) 10–18. doi:10.1016/J.CULHER.2017.07.004.

Figure captions:

Fig. 1 – The nineteenth century oil painting "Hunting Scene" (95 x 54 cm) with the Er:YAG laser test areas (A); Laser cleaning in progress (B).

Fig. 2 - Detail of one tests (one scan, 2.1 J/cm^2). At top left the dry irradiated area is shown, followed by other irradiated areas pre-wetted with the following solutions: deionised water (DIW), 1% v/v Tween20 in DIW, 50% v/v Industrial Methylated Spirit (IMS) in DIW, 50% v/v IMS in White Spirit and White Spirit. All the laser irradiated areas were 15x15 mm.

Fig. 3 – ATR/FT-IR spectra of the TTP varnish samples collected on the nineteenth century painting by scalpel and control dammar (inlet).

Fig. 4 – The Py-TMAH-GC/MS chromatograph that indicates that the varnish of the painting was dammar. The MS spectra are shown in Figs. S3-S10

Fig. 5 - Micrographs of the dry irradiated test areas with a satisfactory outcome. A: One laser scanned area at nominated fluence 2 J/cm^2 and B: two laser scanned area at nominated fluence 0.7 J/cm^2; I) visible light (VL); II) UV induced fluorescence; III) VL stereomicrograph. All the laser irradiated areas studied were 15x15 mm.

Fig. 6 – Micrographs of the DIW+TW20 prewetted irradiated test areas with a satisfactory outcome. A: One laser scanned area at nominated fluence 2.4 J/cm^2, B: two laser scanned area at nominated fluence 2.3 J/cm^2 and C: three laser scanned area at nominated fluence 2.1 J/cm^2; I) visible light (VL); II) UV induced fluorescence; III) VL stereomicrograph. All the laser irradiated areas studied were 15 x 15 mm.

Fig. 7 – UV induced fluorescence of resin fragments collected on glass coverslips upon dry (A) and pre-wet (B) laser irradiation at 1.5 J/cm^2. The glass coverslipls were 15 x 15 mm

Fig. 8 – Gloss related impact due to laser-irradiation (ΔGRF) as a function of nominated fluences. A good correlation of this factor with the disruption of the varnish at these fluences as visually assessed for the dry irradiation tests was observed. In the case of the wet irradiation tests this correlation was less representative, perhaps due to the significantly less material that escaped the irradiated varnish.

Fig. 9 - Multispectral Imaging clusterisation maps of one (A) and two (B) laser scanned areas at nominated fluence 15 J/cm^2. The sequence of the cleaning test areas is the same as in Fig. 2. All the laser irradiated areas shown are 15 x 15 mm.

Fig. 10 - Ratios of average reflectance spectra of red and green clusters, representing reflectance differences due to remaining varnish thickness as reported elsewhere [41].

Fig. 11 – A % clustered reflection monitored by the spectral imaging clusterisation maps as a function of fluence for the two laser scan applications in the dry and pre-wet tests. The gradual reduction of the varnish from the early stage (green line) to the deeper thinning (red line) was captured by spectral imaging. The black line corresponds to the remaining varnish within the irradiated spots.

Fig. 12 – ATR/FT-IR spectra of the resin fragments collected on the glass coverslips, acquired at nominated fluence 1.5 and 2.1 J/cm^2 and of the untreated varnish (control). ATR/FTIR spectra of: the dry irradiated area after two laser scans (A); and the pre-wetted area after three laser scans (B). The spectra show the gradually reduction in intensity of the C=O stretching group by increasing fluence. Baseline points ranging from 3700-3100, 3100-2700, and 1900-1550 cm^{-1}.

Table captions:

Table 1 – Wavenumbers corresponding to the maxima of the IR absorbance bands of the control dammar and the painting varnish [24,26,43].

Table 2 – Molecules recorded via Py-TMAH-GC/MS. The data are in line with findings published elsewhere [16,17,19,24,27,28].

Table 3 – The table provides the $\boldsymbol{L^*_{SCI_{mean}}}$ and $\boldsymbol{L^*_{SCE_{mean}}}$ and the GRF data before and after laser irradiation and the ΔGRF values. Standard deviations (σ) of all data are provided. Data in **bold** represent the least efficient visually assessed outcome. <u>Underlined</u> data represent an acceptable level of irradiation of the varnish with no identification of brown hue of the laser scanned area.

Table 4 - Multispectral Imaging (MSI) Clusterisation Analysis data of the Er:YAG laser irradiated areas. Green % corresponds to a gradual reduction of the early stage varnish thinning. Red % coincides with gradual deeper irradiation of the varnish layer. The Black % corresponds to the remaining varnish within the irradiated spots.

dammar Wavenumbers (cm^{-1})	Triterpenoid varnish painting sample Wavenumbers (cm^{-1})	Band assignment
3400	3400	ν_s O–H
2930	2943	ν_{as} CH_3/CH_2
2867	2875	ν_s CH_3
1705	1705	ν C=O (aldehydes, ketones and carboxylic acids)
1640	1630	ν C=C of cis –C=C–
1453	1453	δ CH_3/CH_2
1379	1380	δ CH_3
1250	1236	ν C–C vibration, δ C–H in ring
1178	1165	δ C–H in ring, ν C–O in esters, ν C–C in alkanes
1026	1033	δ C–H in ring, ν C–O
923	-	C–H out-of-plane deformation, (one only H attached to ring)
891	874	C–H out-of-plane deformation, (two adjacent H attached to ring)

Table 1

Retention Time (min)	Compound	Molecular structure	MW	m/z	Figure
45.3	dammaradienone	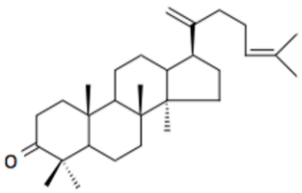	424	109, 189, 205	S2
46.3	dammaradienol	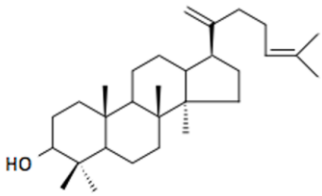	426	109, 207	S3
49.5	dammarenolic acid	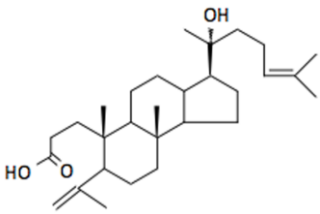	472	109, 454	S4
53	oleanonic acid	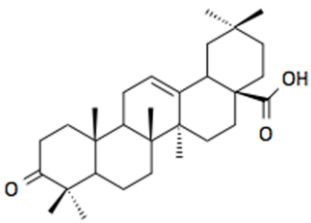	548	143	S5

54	hydroxydammarenone (3-oxo-dammara-20,24-diene)	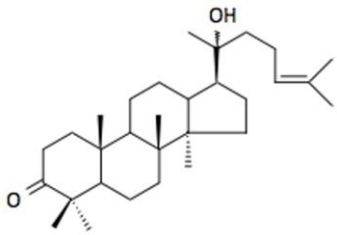	442	109, 205, 424	S6
55.5	oleanonic aldehyde	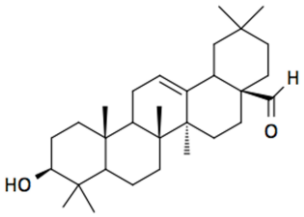	409	189,203,232	S7
55.6	ursonic acid	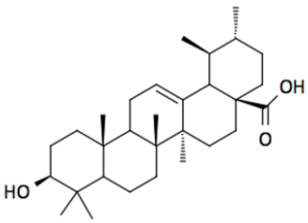	468	205	S8
56.4	ursonic aldehyde	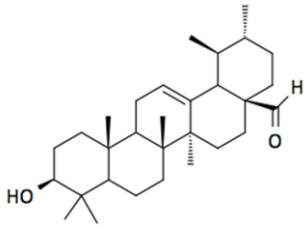	438	133, 203, 232,409	S9

Table 2

Energy (mJ)	Nominated Fluence (J/cm^2)	Cleaning Systems	Colourimetry before laser irradiation			Colourimetry after laser irradiation			ΔGRF ± σ
			$L^*_{SCI_{mean}}$ ± σ	$L^*_{SCE_{mean}}$ ± σ	GRF_b ± σ	$L^*_{SCI_{mean}}$ ± σ	$L^*_{SCE_{mean}}$ ± σ	GRF_a ± σ	
40	**0.6**	Dry – 1 Scan	42 ± 0.6	40 ± 0.7	2 ± 0.1	43 ± 1.1	43 ± 1.3	1 ± 0.2	1 ± 0.1
		Dry – 2 Scans	32 ± 0.5	31 ± 0.1	1 ± 0.2	36 ± 0.9	36 ± 1	0.3 ± 0.1	1 ± 0.1
		DIW+TW20 – 1 Scan	39 ± 0.5	38 ± 0.2	2 ± 0.2	44 ± 0.6	44 ± 0.6	0.4 ± 0.0	1 ± 0.1
		DIW+TW20 – 2 Scans	32 ± 1.3	31 ± 1.3	1 ± 0.0	37 ± 0.7	37 ± 0.7	0.2 ± 0.0	0.4 ± 0.0
		DIW+TW20 – 3 Scans	33 ± 2.8	31 ± 2.7	2 ± 0.1	40 ± 0.6	39 ± 0.6	1 ± 0.0	1 ± 0.0
50	**0.7**	Dry – 1 Scan	32 ± 1.3	30 ± 1.3	2 ± 0.0	38 ± 0.1	37 ± 0.1	0.3 ± 0.0	1 ± 0.0
		Dry – 2 Scans	31 ± 0.3	31 ± 0.4	0.5 ± 0.1	38 ± 0.8	37 ± 0.8	0.1 ± 0.0	0.4 ± 0.0
		DIW+TW20 – 1 Scan	35 ± 1.7	33 ± 1.3	2 ± 0.3	43 ± 1.2	42 ± 1.2	1 ± 0.0	1 ± 0.2
		DIW+TW20 – 2 Scans	31 ± 0.5	31 ± 0.6	0.5 ± 0.1	37 ± 1.1	37 ± 1.1	0.1 ± 0.0	0.3 ± 0.0
		DIW+TW20 – 3 Scans	30 ± 1.0	27 ± 1.0	3 ± 0.0	35 ± 0.3	34 ± 0.3	1 ± 0.0	3 ± 0.0
70	**1**	Dry – 1 Scan	35 ± 1.9	33 ± 1.9	2 ± 0.0	43 ± 0.7	42 ± 0.6	0.2 ± 0.0	2 ± 0.0
		Dry – 2 Scans	34 ± 3.4	32 ± 2.3	1 ± 0.8	35 ± 0.7	35 ± 0.9	0.2 ± 0.2	1 ± 0.4
		DIW+TW20 – 1 Scan	38 ± 1.9	36 ± 2.5	2 ± 0.4	39 ± 3.2	38 ± 3.3	1 ± 0.1	1 ± 0.2
		DIW+TW20 – 2 Scans	34 ± 0.8	32 ± 0.4	1 ± 0.2	38 ± 0.6	38 ± 0.6	0.3 ± 0.0	1 ± 0.1
		DIW+TW20 – 3 Scans	34 ± 3.4	32 ± 4.1	2 ± 0.5	37 ± 0.9	36 ± 0.9	0.5 ± 0.0	1 ± 0.3
110	**1.5**	**Dry – 1 Scan**	**32 ± 1.3**	**30 ± 1.6**	**2 ± 0.2**	**37 ± 0.4**	**37 ± 0.4**	**0.2 ± 0.0**	**2 ± 0.1**
		Dry – 2 Scans	32 ± 1.1	32 ± 0.9	1 ± 0.2	38 ± 0.2	38 ± 0.2	0 ± 0	1 ± 0.1
		DIW+TW20 – 1 Scan	32 ± 1.2	31 ± 1.6	1 ± 0.2	41 ± 1.4	41 ± 1.4	0.2 ± 0.0	1 ± 0.2
		DIW+TW20 – 2 Scans	34 ± 1.8	33 ± 1.5	1 ± 0.2	38 ± 0.5	38 ± 0.5	0.1 ± 0.0	1 ± 0.1
		DIW+TW20 – 3 Scans	32 ± 0.7	30 ± 0.8	1 ± 0.1	33 ± 1.7	33 ± 1.7	0.5 ± 0.0	1 ± 0.0
140	**2**	Dry – 1 Scan	35 ± 4.3	30 ± 2.6	5 ± 1.2	40 ± 0.2	40 ± 0.2	0.2 ± 0.0	5 ± 0.8
		Dry – 2 Scans	**35 ± 0.7**	**34 ± 0.8**	**1 ± 0.1**	**39 ± 0.9**	**38 ± 0.9**	**0.2 ± 0.0**	**1 ± 0.1**
		DIW+TW20 – 1 Scan	28 ± 4.5	25 ± 4.7	4 ± 0.1	36 ± 0.4	36 ± 0.3	0.3 ± 0.1	3 ± 0.0
		DIW+TW20 – 2 Scans	35 ± 0.5	34 ± 0.5	1 ± 0.0	39 ± 1.2	39 ± 1.2	0.1 ± 0.0	1 ± 0.0
		DIW+TW20 – 3 Scans	32 ± 1.8	30 ± 2	2 ± 0.1	35 ± 0.8	35 ± 0.8	0.3 ± 0.0	1 ± 0.1
150	**2.1**	**Dry – 1 Scan**	**33 ± 0.1**	**31 ± 0.5**	**2 ± 0.2**	**39 ± 0.3**	**39 ± 0.3**	**0.2 ± 0.0**	**2 ± 0.2**
		Dry – 2 Scans	**36 ± 0.6**	**36 ± 0.6**	**1 ± 0.0**	**39 ± 1.3**	**38 ± 1.3**	**0.1 ± 0.0**	**1 ± 0.0**
		DIW+TW20 – 1 Scan	35 ± 2.8	33 ± 2.7	2 ± 0.1	39 ± 1.1	39 ± 1.1	0.2 ± 0.0	2 ± 0.1
		DIW+TW20 – 2 Scans	35 ± 1.3	34 ± 1.4	0.5 ± 0.1	37 ± 1.2	37 ± 1.2	0.1 ± 0.0	0.3 ± 0.1
		DIW+TW20 – 3 Scans	31 ± 1.0	29 ± 0.8	2 ± 0.1	31 ± 0.5	30 ± 0.5	1 ± 0.0	1 ± 0.1
160	**2.3**	**Dry – 1 Scan**	**31 ± 2.0**	**28 ± 2.4**	**3 ± 0.3**	**42 ± 0.1**	**42 ± 0.1**	**0.1 ± 0.0**	**3 ± 0.2**
		DIW+TW20 – 1 Scan	30 ± 1.3	27 ± 1.4	3 ± 0.1	36 ± 0.8	36 ± 0.8	0.2 ± 0.0	2 ± 0.0
		DIW+TW20 – 2 Scans	35 ± 2.0	33 ± 2.4	2 ± 0.3	39 ± 0.6	39 ± 0.5	0.2 ± 0.0	1 ± 0.1
170	**2.4**	**Dry – 1 Scan**	**32 ± 2.4**	**31 ± 2.7**	**1 ± 0.3**	**39 ± 0.4**	**38 ± 0.4**	**0.1 ± 0.0**	**1 ± 0.2**
		DIW+TW20 – 1 Scan	30 ± 0.6	29 ± 0.6	1 ± 0.0	37 ± 0.7	38 ± 0.7	0.1 ± 0.0	1 ± 0.0
		DIW+TW20 – 2 Scans	35 ± 0.9	35 ± 0.9	0.3 ± 0.0	39 ± 0.5	39 ± 0.5	0.1 ± 0.0	0.2 ± 0.0

Table 3

Energy (mJ)	Nominated Fluence (J/cm^2)	Cleaning systems	Spectral Imaging Clusterisation Analysis		
			Green %	Red %	Black %
40	**0.6**	Dry – 2 Scans	88	9	3
		DIW+TW20 – 2 Scans	84	14	2
		DIW+TW20 – 3 Scans	23	76	1
50	**0.7**	Dry – 2 Scans	8	92	0
		DIW+TW20 – 2 Scans	69	26	5
		DIW+TW20 – 3 Scans	80	16	4
70	**1**	Dry – 2 Scans	17	83	0
		DIW+TW20 – 2 Scans	72	19	9
		DIW+TW20 – 3 Scan	19	81	0
110	**1.5**	Dry – 1 Scan	25	75	0
		Dry – 2 Scans	31	69	0
		DIW+TW20 – 1 Scan	45	45	10
		DIW+TW20 – 2 Scans	41	58	1
		DIW+TW20 – 3 Scans	66	34	0
140	**2**	Dry – 1 Scan	29	70	1
		Dry – 2 Scans	6	94	0
		DIW+TW20 – 1 Scan	46	52	2
		DIW+TW20 – 2 Scans	5	95	0
		DIW+TW20 – 3 Scans	66	34	0
150	**2.1**	Dry – 1 Scan	8	91	1
		Dry – 2 Scans	3	97	0
		DIW+TW20 – 1 Scan	12	88	0
		DIW+TW20 – 2 Scans	14	86	0
		DIW+TW20 – 3 Scans	71	12	17
160	**2.3**	Dry – 1 Scan	4	96	0
		DIW+TW20 – 1 Scan	33	67	0
		DIW+TW20 – 2 Scans	9	91	0
170	**2.4**	Dry – 1 Scan	12	88	0
		DIW+TW20 – 1 Scan	40	60	0
		DIW+TW20 – 2 Scans	29	71	0

Table 4

Notes

[a] The spectrometer was equipped with a Universal Attenuated Total Reflection (UATR) single polarization accessory using a pure diamond ATR unit. The spectrometer was part of the Spotlight 400N FT-NIR Imaging System.

[b] The nominated fluences used during this study were: 0.6 J/cm^2, 0.7 J/cm^2, 1 J/cm^2, 1.5 J/cm^2, 2 J/cm^2, 2.1 J/cm^2, 2.3 J/cm^2, 2.4 J/cm^2.

[c] Tween 20: Polyoxyethylenesorbitan monolaurate supplied by Sigma Aldrich

[d] Supplied by Thermo Fisher scientific. Methylated spirit industrial 74 O.P.. Component: Ethyl alcohol > 94%; Methyl alcohol 3- 6%; Water 1%.

[e] Sigma Aldrich

[f] The interactive solvent and solubility triangle© - http://www.icr.beniculturali.it/flash/progetti/TriSolv/TriSolv.html

[g] Fractional Solubility Parameter for: a) DIW was Fd 18 (non polar dispersion force - Van der Waals or instant dipole), Fp 28 (polar dipole force - permanent dipole), Fh 54 (hydrogen bonding force); b) 50% IMS+DIW was Fd 26.82, Fp 23.12, Fh 50.06; c) 50% IMS+WS was Fd 62.82, Fp 11.12, Fh 26.06; d) WS was Fd 90, Fp 4, Fh 6.

[h] http://www.tipp.gr, 10/2017.

[i] All the data were imported in TIPP, and the raw spectral cube was created for both the test areas images and the white reference images. Using the XpeEye acquisition software, the contribution of the dark current was removed a priori from both the test areas and DRT images. Subsequently, the sample's spectral cube was normalised by a TIPP module, correcting the spectral intensity profile and any unevenness of the light across the test areas. This was achieved by dividing the sample's spectral images (with the relative DRT's spectral images and multiplying) with the known reflectivity of the DRT at each wavelength band investigated. Registration was conducted by a custom-made algorithm specifically designed to operate with data derived from multi-spectral imaging systems [44].

[j] This specific effect was clearly visible at naked eye but, in this case, it was not recorded with OM and SEM techniques (mainly due to the size of the painting).

[k] The full set of data generated from the tests were not provided in this paper. Please refer to the corresponding author if needed.